Energy of Fluid foams

Y. Jiang[a], F. Graner[b], E. Janiaud[c], and C. Flament[c1, 2, 3]

[1a] *Theoretical Division, Los Alamos National Laboratory, Los Alamos, New Mexico 87545, U.S.A.*

[2b] *CNRS UMR 5588 et Université Grenoble I, Laboratoire de Spectrométrie Physique, BP 87, F-38402 St Martin d'Hères Cedex, France.*

[3c] *Laboratoire des Milieux Désordonnés et Hétérogènes, case 78, Université Paris 6 and CNRS UMR 7603, 4 place Jussieu, 75252 Paris Cedex 05, France, and Université Paris 7, Denis Diderot, Unité de Formation et de Recherche de Physique (case 70.08), 2 place Jussieu, 75051 Paris Cedex 05, France.*

Foam's mechanical properties depend on its structures. Based on foam's geometrical and topological characteristics, we study the stable and metastable energies of two-dimensional foams with fixed areas. We present a theoretical estimate of the ground state energy. We then treat the contributions from area polydispersity, topological charges and boundary conditions as perturbations to the honeycomb structure which has the absolute minimum energy, and obtain the equilibrium energies for arbitrary foam patterns. Using a novel annealing techniques, we study the energies of ferro-fluid foams (FFF) during a relaxation from a highly distorted state to nearly the global energy minimum. We also study energy relaxation in a Monte Carlo model (the extended large-Q Potts model). Results from both FFF and simulations support our theory.

I INTRODUCTION

Fluid foams are a class of materials, including soap foams, emulsions, magnetic garnets, which consists of a collection of cells tending to minimize their surface energy. In their various industrial applications, ranging from food and shaving cream to fire fighting and oil recovery [1, 2, 3], foams' mechanical properties play an important role but have not yet been well understood. Foams support small stress like a solid, but flow like a fluid under sufficiently large shear, when the bubbles rearrange from one metastable configuration to another. This solid-like to fluid like transition depends sensitively on the foam structure [4]. Hence understanding their structure is an important step towards predicting foam's mechanical properties, e.g. the quasistatic stress-strain relationship.

Due to the opaqueness of foams, the structure and the bubble-level processes in three-dimensional foams are difficult to visualize. Thus two-dimensional foams, which are both experimentally and theoretically more tractable, becomes a good starting point for building the foundation to bridge structure and properties. Contrary to the common believe that 2D foam structure is well understood, we think our knowledge is far from complete. On the one hand, rigorous proof exists thus far only for a few most simple cases such as perfectly ordered (honeycomb lattice [5]) or trivial (one, two and three bubbles) structures [6, 7, 8, 9, 10]. On the other hand, many empirical rules such as the Aboav-Weaire law have been gethered for real foams but lack explanations. This paper bases on these well known results to study the energy of 2D foams, aiming at using a physicist's insight to generalize the understanding from simple cases to the realistic foams.

We start from the two-dimensional foams with fixed areas, i.e. foams are non-coarsening and incompressible [11]. Since the macroscopic properties depend on the static structure, coarsening is only a secondary complication which can be included as time dependent length scale. In general, the mechanical response of foams is of a timescale much shorter that that of coarsening, e.g. in flowing foams, we can neglect the effects of coarsening. We also choose the neglect the compressibility of foams as its not essential to fluid foams.

The structural characteristics of equilibrium foams are described by the Plateau's rules. First, bubbles are in contact with one another with no interstitial spaces, or bubbles are space-filling; second, bubble edges are circular arcs, which meet by 3 at $2\pi/3$ angles, hence by virtue of Euler's theorem, the average number of bubble neighbors is six in foams without boundaries (infinite or with periodic boundary conditions); third, the total curvature of the edges around a vertex is zero [10].

We use two model foams that satisfy the Plateau's rules at equilibrium for our study. This paper is organized as follows. The next session introduces the model foams: 2D ferrofluid foams and simulated foams with the extended large-Q Potts model. Both foams have constant bubble areas thus eliminate the unwanted coarsening and enable us to study the stable and meta-stable energies of 2D foams. Session III describes our theoretical description of foam energy and compares the theoretical predictions with results from FFF and simulations. The last session summarizes our results and conjectures the implications and potential applications of this work.

II MODEL FOAMS

The detailed description of FFF has appeared in [12]. An FFF is made from an immiscible mixture of an ionic magnetic fluid (13% aqueous black magnetic liquid) and oil (87% white-spirit). The fluid mixture is trapped in the 1 mm space between two

parallel plexiglass plates. A homogeneous magnetic field of 9 kA/m perpendicular to the plates induces the cellular structure and fixes the bubble edge thickness [12]. The magnetic dipolar interaction is much weaker than the surface tension, thus the equilibrium foam pattern minimizes its surface energy. Figure 1a shows an equilibrium FFF picture with the dark lines formed by the magnetic fluids. The bubbles are surrounded by the same oil as that filled the bubbles, corresponding to a free boundary condition. The area distribution is fixed by nucleation conditions [12]. We tilt the plexiglas plates from the horizontal plane to an angle of $0.1°$, large bubbles drift upwards, small bubbles downwards, resulting in size-sorting [13]. Then we bring the plates back to horizontal, bubbles slowly drift and settle. This procedure allows the bubbles to rearrange and explore the energy space to find a lower energy configuration. The final stable pattern, Fig. 1a corresponds to an equilibrium energy state. Figure 1b shows an FFF at different stages of relaxation.

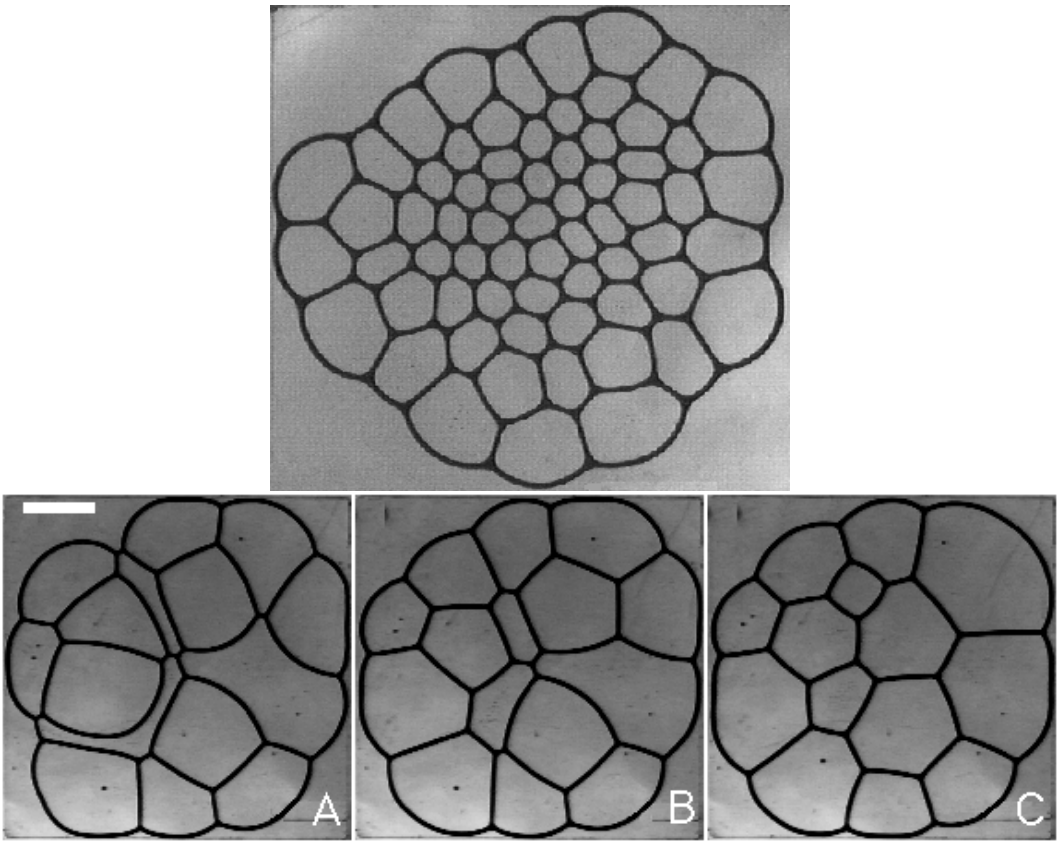

FIG. 1: Ferrofluid foams with fixed areas: (a) Annealed FFF image with $N_b = 19$ bubbles at the free boundary, topological charge $Q = 25$, area dispersity $\delta A = 0.443\bar{A}$, and wall thickness $e = 0.126\bar{A}^{1/2}$. (b) A. Freshly nucleated FFF with highly distorted bubbles. B. After a relaxation which involved an avalanche of bubble rearrangements. C. After a few bubble rearrangements induced by perturbing the foam. Scale bar in A indicates 10mm.

The other model we study is the simulated foam from the extended large-Q Potts model [4]. This model treats a 2D foam on a 2D lattice by assigns an integer number to each lattice site. Domains of like numbers are bubbles with the bubble walls described by the differences of bubble numbers. Each unmatching pair of numbers contributes to the bubble wall surface energy, thus energy minimization through a Monte Carlo process results in minimal bubble perimeters. An area constraint keeps the bubble areas constant. This model simulates foams in the dry limit. Figures 2a, 2b and 2c show respectively foam patterns with periodic and fixed boundary conditions, and a polydispersed foam. Note that with fixed boundary conditions, bubble edges at the boundaries are perpendicular to the boundaries.

III FOAM ENERGY

Such equilibrium configurations, Fig 1 and 2, are characterized by the topology and the geometry. The topology refers to the list of neighbor relations, from which one can deduce the number of vertices n_i of bubble i or equivalently its "topological

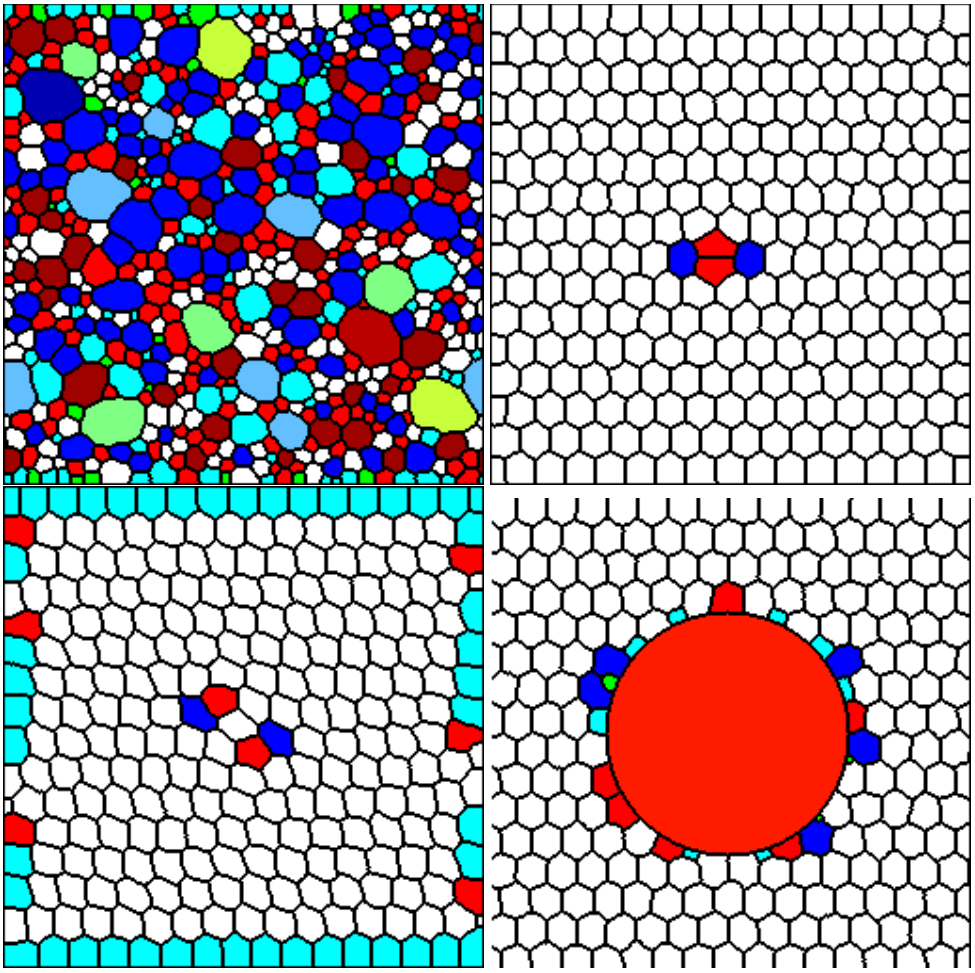

FIG. 2: Simulated foams with fixed areas: (a) A typical configuration of a polydispersed foam at equilibrium. The boundaries are fixed in the vertical direction and periodic in the horizontal direction. The lattice is 256×256 with 589 bubbles. Colors encode the topological charges. The area dispersity is $\delta A/\bar{A} = 1.06$. (b) An artificially constructed foams with equal areas ($\delta A/\bar{A} = 0.4\%$) and periodic boundaries. A pentagon-heptagon-pentagon-heptagon cluster forms a topological quadrupole, with the rest of the honeycomb lattice undisturbed. (c) Two dipoles (pentagon-heptagon pair) result in a curvature field in the hexagons around them. (d) A foam illustrating the fix boundary conditions: a circular boundary in the center of a hexagon foam induces a topological charge distribution in the bubbles touching the boundary, notice all the edges are perpendicular to the solid boundary.

charge", $q_i = 6 - n_i$. And the geometry includes the angle and length of the edges and their algebraic curvature κ_{ij} ($\kappa_{ij} = -\kappa_{ji} > 0$ when i is convex). The energy of a foam with N bubbles is:

$$H = \gamma \sum_{i=0}^{N} L_i = 2\gamma \sum_{i \le j} \ell_{ij}, \tag{1}$$

where γ is the line tension of bubble edges, L_i is the perimeter of bubble i, ℓ_{ij} is the length of the edge between bubbles i and j, $i = 0$ corresponds to the boundary. The factor 2 comes from that each edge is counted twice because it has two edge-fluid and inner-fluid interfaces.

If all bubbles have equal areas, the minimal energy corresponds to the regular hexagonal lattice or the honeycomb structure [5]. In [14], we have estimated the ground energy, H_0 by a perturbation around the ideal regular hexagon lattice:

$$H_0 = H_h + H_e + H_t + H_b, \tag{2}$$

where the labels stand respectively for "hexagon", "epitaxy", "topological defect", and "boundary".

The energy $H_h = \bar{L} = \sqrt{\bar{A}}$ is exact for the regular hexagonal lattice. But when the areas are not equal, $H_h = (\gamma/2)\sum_{i=1}^{N} 2\sqrt{\pi_6 A_i}$ is a good zeroth-order estimate for H_0, where $\pi_6 = 2\sqrt{3}$ is the isoperimetric constant for a regular hexagon.

This estimate is tested with the model foams. We can prepare highly distorted FFF foams as initial conditions (Fig. 1b A) where the edge lengths, bubble elongation and the topologies all have wide variations. To minimize their surface energy, the distorted foams spontaneously undergo an avalanche of bubble rearrangements or "T1"' processes, and reach the metastable states with lower energy. We can then perturb the foams by perturbing the vertices using a magnetic pin [15], forcing the energetically favorable T1 processes to occur and the bubbles to settle into configurations with even lower energy. Figure 3a shows the energies during this relaxation process. For all five trials, the final energies of the relaxed foams are rather close to the estimate H_h (or $H : H_h \approx 1$).

In simulations, by biasing the Monte Carlo probabilities in the direction of shear, we can apply shear to a foam [4]. Higher shear rates result in more distorted foams thus higher energies. Using these deformed foams as initial conditions, we allow the foams to relax towards equilibrium configurations. Figure 3 shows that the fully relaxed foams all have energies close to the ground energy, regardless the initial energies. However, increasing the resolution of the data (inset of Fig. 3), we see that the higher initial energies relax to lower final energies. This can be understood if we consider that the more distorted foams have more chances during their relaxation to explore the energy landscape, and thus can reach lower energy states.

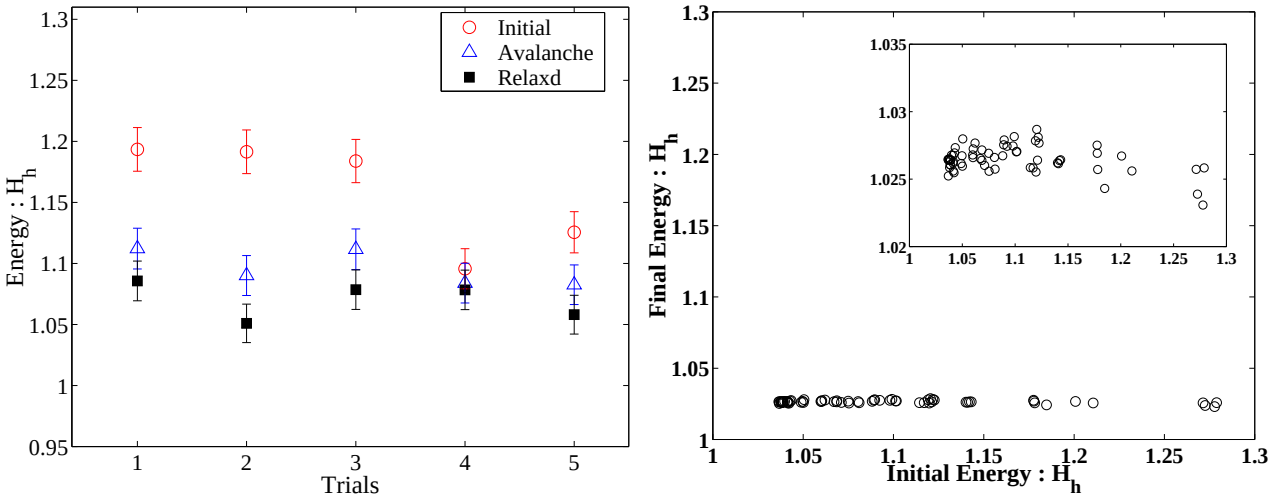

FIG. 3: Ratio of energy H of a relaxed foam from simulations of one foam, to the energy H_h of a collection of regular hexagons with the same area distribution Energies of the relaxed foam from different initial energy. The inset shows the same data by enlarging the scale of y axis 20 times.

The first correction to the foam energy comes from the epitaxy of bubbles of different sizes. When two square with areas $A_i \neq A_j$ are in contact, the edge they share must have a length between $L_i = \sqrt{A_i}$ and $L_j = \sqrt{A_j}$. In fact, to minimize the perimeter while keeping the areas the same, the optimal length for the edge they share must be $L = \sqrt{L_i L_j}$. The resulting

energy cost due to the lattice mismatch, i.e. the strain energy, is proportional to $\gamma[(L_i - L_j)/(L_i + L_j)]^2$ [16]. This result holds for a square or rectangular lattice. We now generalize the result to arbitrary configurations with small area differences, the optimal edges being $L_{ij} \equiv \sqrt{L_i L_j}$ with $L_i \equiv \pi_n A_i$, where π_n is the isoperimetric constant for a polygon of sides n. The energy contribution is $H_e = \gamma \sum_{ij}[(L_i - L_j)/(L_i + L_j)]^2$. In a macroscopic description this becomes $\sim \gamma \int d^2\vec{r}(L/A)(\vec{\nabla}A/A)^2$, with an additional term $\sim \hat{n} \cdot \vec{\nabla}\ (\vec{\nabla}A \cdot \hat{n})$ coupling the area repartition with the local orientation $\hat{n}$ of the (now distorted) hexagonal lattice. For an interface between two hexagonal lattices, these two terms respectively provide a line tension and a spontaneous curvature. Thus H_e requires a sorting of bubbles according to their size to lower the energy. In a foam with free boundaries, larger bubbles tend to sort outwards, as shown in Fig 1a, where bubbles are radially sorted according to their sizes, larger bubbles in the outer region.

The optimal length between bubble i, j of areas A_i and A_j is L_{ij} corresponds to configurations with an equilibrium energy. The difference of actually length ℓ_{ij} thus indicates the distance of the actually configuration from the equilibrium. During a relaxation, ℓ_{ij} should relax towards L_{ij} if our conjecture is correct. We test this conjecture by measuring ℓ_{ij}/L_{ij} in both FFF and simulated foams.

Figure 4a shows the dependence of the standard deviation $\delta\ell_{ij}/L_{ij}$ as a function of the energies of FFF during the same relaxations as in Fig 3a. The foam energy relaxes towards H_h progressively. The energies for the fully relaxed foams remain slightly higher than H_h, because the bubbles cannot all become hexagons, supporting that H_h is the lower bound for foam energy. The mean value of ℓ_{ij}/L_{ij} is close to 1 (data not shown) with the standard deviation tend towards zeros as the foams relax. The deviation of the real edge length ℓ from L_{ij} reflects local deviation from equilibrium. The more distorted the foam is, the more edges would be away from the equilibrium value of L_{ij}. Thus the same trend in both $H : H_b$ and $\delta\ell_{ij}/L_{ij}$ indicate that during relaxation the foam relaxed *globally* and *locally* towards equilibrium.

Figure 4b shows the histograms of ℓ_{ij}/L_{ij} for a relaxation of the simulated foam at several relaxation times. The distribution of ℓ_{ij}/L_{ij} becomes narrower as the foam relaxes, and the average of the distribution shifts towards 1. In comparison with the FFF data, Fig. 4c plots the standard deviation, $\delta\ell_{ij}/L_{ij}$, the width of the distribution, during relaxations for the same foam as in Fig. 3b as well as several other foams with different boundary conditions and area distributions. All foams show the same trend in energy and the deviation, showing both *global* and *local* equilibration, agreeing qualitatively with FFF results shown in Fig 4a.

The second correction to the energy of hexagons comes from topological charges. An isolated topological charge does not cost energy by itself, but it creates a pressure gradient and hence a curvature field. This is evident in Fig. 2b and 2c. In Fig 2b, a topological quadrupole does not affect the rest of the honeycomb lattice, while in Fig 2c two pairs of dipoles deform their neighboring bubbles and induce curved edges in the hexagons around them. The energy contribution from the curvature field is the sum over all curved edges:

$$H_t \approx 2\gamma \sum \frac{\ell_{ij}^3 \kappa_{ij}^2}{24}. \tag{3}$$

The summation involves the electrostatic-analogy calculation [14]. For a single topological charge (i.e. a defect or dislocation), we find that H_t grows logarithmically with the size of the foam, as expected in analogy with the self-energy of a single 2D electrostatic charge. Thus for a large foam, a single topological charge costs so much energy that it is unlikely to exist isolated. Topological charges tend to aggregate. For two charges q, q' separated by a distance $r \gg L$, the energy is $H_t = -(qq'A/2\pi\epsilon_{eff}) \ln(r/L)$. Two opposite charges $-q, +q$ (e.g. a pentagon-heptagon pair) a distance $d \sim L$ apart have a dipolar moment $\vec{p} = q\vec{d}$ and create a dipolar potential $P(\vec{r}) = q\vec{d} \cdot \vec{r}/(2\pi\epsilon_{eff} r^2)$ which can in turn interact with another dipole (Fig. 2b) to form a quadrupole, and so on. We can then apply the electrostatics analogy to calculate their energies. The potential energy (pressure field) for a foam with multiple charges is simply the superposition of those for every single charges.

As real foams are neither infinite nor having periodic boundary conditions, we consider the energy contribution from the free or fixed boundaries. The Gauss-Bonnet theorem [17] states that the charged Q enclosed by a contour is $Q = 6 - v_+ + v_-$, where v_+ and v_- are the number of vertices pointing outwards and inwards, respectively. Apply it to the boundary of the foam, for which $v_+ = 0$ and $v_- = N_b$, (except of course in the trivial case where there is a single bubble, $N_b = 1 \neq v_- = 0$), we find that the total charge of a foam is $Q = N_b + 6$.

The energy contribution from the boundary conditions, H_b is a function of the number of bubbles at the boundary, N_b. Periodic boundary conditions warrant that the total charge $Q = 0$ and $N_b = 0$, thus contribute no energy. For real foams, we have found it more convenient to handle the "effective charge" $q' = q = 6 - n$ for bubbles not touching the foam boundary, and $q' = q - 1 = 5 - n$ for bubbles at the foam boundary. Then the total Q' over a foam is 6, see Fig. 2b.

For a free foam, the pressure obeys a Poisson-type equation, the sources being the effective charge q', the boundary condition for the pressure field being $P \equiv P_0$. This is a Dirichlet problem, thus it has a unique solution. The energy H_b due to the boundary itself can be calculated [14]; for large N it writes:

$$H_b \sim \gamma \frac{N_b L}{6} \left(\frac{2\pi}{\pi_6} - 1 \right). \tag{4}$$

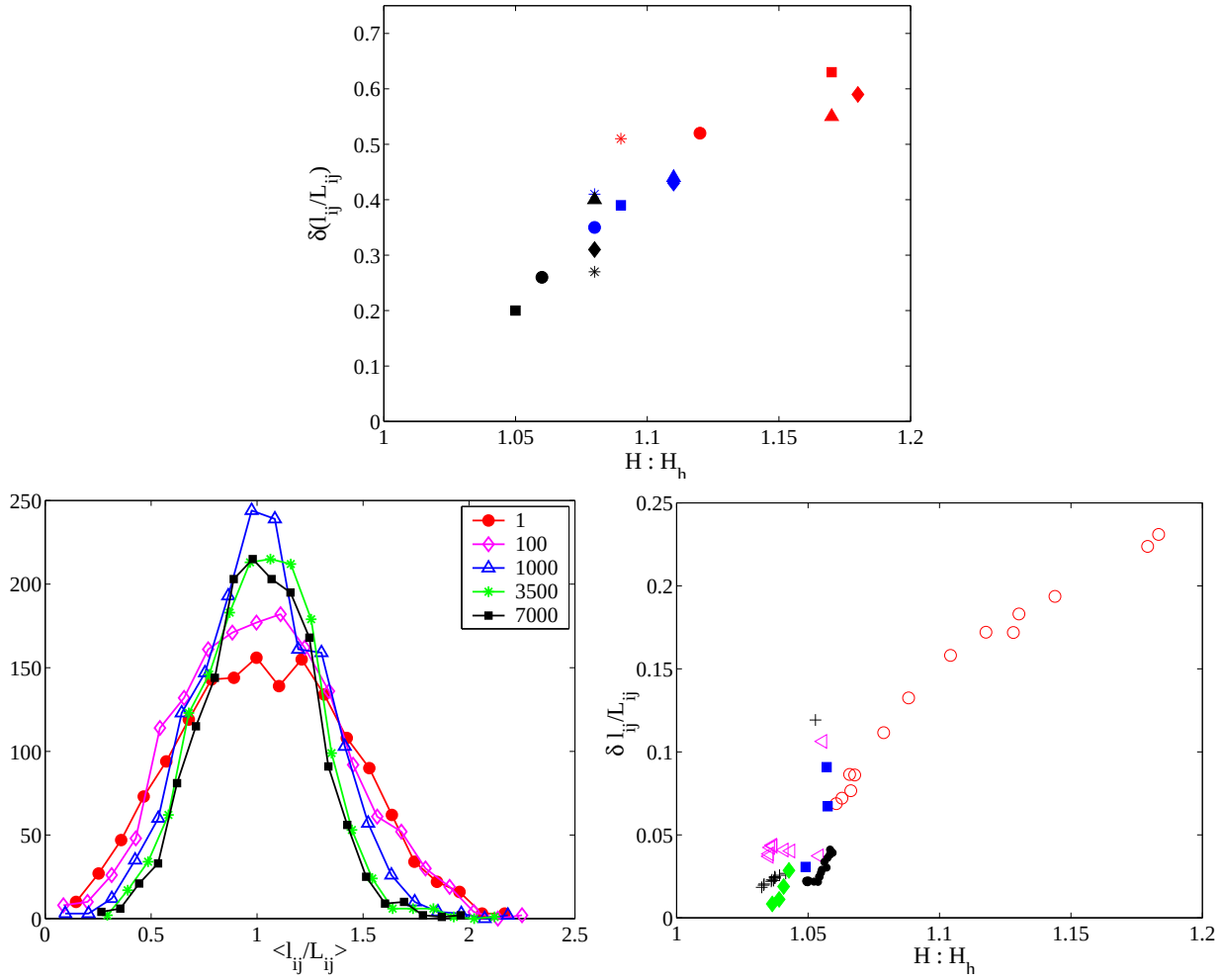

FIG. 4: Data ℓ_{ij}/L_{ij}. (a) FFF experiment data for the standard deviation $\delta\ell_{ij}/L_{ij}$. (b) Simulated foam, standard deviation to $H : H_h$. Circles correspond to the same foams as in Fig. 2a, a polydispersed foam with lattice size 256×256 and 585 bubbles; squares, pluses, triangles, diamonds and bullets correspond to different foams with various bubble sizes and area distributions: the wider the area distribution corresponds to larger $\delta\ell_{ij}/L_{ij}$ and higher energy.

Fixed boundary conditions (Fig. 2c) are more difficult to treat exactly. Bubble edges are perpendicular to the boundaries [18], thus the geometry of the boundaries impose a curvature field adding to the curvature field of the foam [19].

IV CONCLUSION

In summary, aiming at bridging the microscopic structure of foams with their macroscopic mechanical responses, we have chosen to study the energy landscape of foams. A detailed description of the energy landscape (free or potential) provides both the static and the quasi-static information of the foams. We study the local and global equilibrium energies for two-dimensional non-coarsening foams based on their geometries and topologies. We have used an analogy with crystals, treating the foam energy by small perturbations around its ground state, the energy of honeycomb structure. This approach allows us to separate the energy contributions from different sources: topology, area polydispersity, and boundaries, and *ab initio* determine the foam energy. We compare the theoretical conjectures with FFF experiments and Potts model simulations, both tools have unique advantages that are beyond many other methods. FFF experiments can have global and local annealing, thus allowing relaxation from highly distorted foams with high energy to completely relaxed foams with energy reaching the ground energy. Potts model offers controlled polydispersity, large number of bubbles for good statistics. The theoretical analysis, combined with the experiments and computer simulations, has given us the opportunity to go beyond description of foam phenomena and gain physical insights.

We have demonstrated that the difference between H and H_h assay quantitatively how far the foam is from its ground state. The difference between ℓ_{ij} and L_{ij} reflects the local deviation from equilibrium, or the local deformation. Use L_{ij} as the reference, we can then define locally for each edge the deformation as e.g.

$$\epsilon = \frac{\ell_{ij} - L_{ij}}{L_{ij}}$$

. We can then measure directly from the foam images both the stress and strain tensor locally and derive from which the stress-strain relationship. We are currently testing this idea with two-dimensional distorted quasi-static foams [20].

The topological contribution H_t shows that a single topological charge costs such a high energy that it is unlikely to appear isolated; two charges of opposite sign tend to get closer. This is enough to explain the origin of the correlations between bubbles, i.e. Lewis and Aboav-Weaire laws [21]. Our estimate of the ground state energy also opens a new avenue for numerical and *ab initio* theoretical studies of energy stored in foams under external stress, and thus helps understand the quasistatic mechanical response under shear, uniaxial compression or gravity field.

Our approach applies to all "perimeter minimizing" systems, including grain boundaries in metals, biphasic fluids and magnetic garnets. We anticipate that the exact calculations presented here might in the future provide a deeper understanding of solid foams produced from their melt, and an archetype on which to build theories for more complex, non-computable heterogeneous systems.

Acknowledgments: We have benefited from friendly discussions with T. Charitat, F. Elias, J.A. Glazier, P. Swart. We would like to thank T. Aste, J. Foisy, F. Morgan, N. Rivier, R. Robert, G. Schliecker, D. Weaire who provided us with articles or preprints prior to publications. YJ is supported in part by DOE under contract W-7405-ENG-36.

REFERENCES

[1] Foams and emulsions, Sadoc and Rivier eds, Cargese. Rivier, Order and disorder 93. Stavans 93. Glazier and Weaire 92

[2] D. L. Weaire, S. Hutzler (eds), Physics of Foams, Oxford Univ Press, 1999.

[3] J. A. Glazier, Ph.D. dissertation, University of Chicago, 1989, unpublished.

[4] Y. Jiang, P. J. Swart, A. Saxena, M. Asipauskas, and J. A. Glazier, Hysteresis and avalanches in two-dimensional foam rheology simulations, Phys. Rev. E **59**, 5819–5832 (1999).

[5] T. C. Hales, The honeycomb conjecture, xyz.lanl.gov/math.MG/9906042.

[6] R. Osserman, The Isoperimetric Inequality, **84**, 1182–1238 (1978).

[7] Almgren 76 ; F. J. Almgren, and J. E. Taylor, Scientific American, **235**, 82 (1976).

[8] H. Howards, M. Hutchings and F. Morgan, The Isoperimetric Problem on Surfaces, Am. Math. Monthly **106**, 430–439 (1999).

[9] F. Morgan, Soap bubbles in $\mathbf{R}^2$ and surfaces, Pac. J. Math. **165**, 347–361 (1994).

[10] J. Foisy, BA thesis unpublished; J. Foisy, M. Alfaro, J. Brock, N. Hodges, and J. Zimba, Pacific J. Maths. **159**, 47–59 (1993).

[11] Bubble areas change over time in real fluid foams. The equilibrium or quasistatic considerations apply to foams on time-scales much shorter than the characteristic variation time $\tau = m/\partial_t m$ of the mass m enclosed in each bubble, of order of hours in FFF like in Fig. 1a.

[12] F. Elias, C. Flament, J.-C. Bacri, O. Cardoso, and F. Graner, Phys. Rev. E 56, 3310 (1997).

[13] F. Elias, J.-C. Bacri, F-H de Mougins, and T. Spengler, Phil. Mag. Lett. 79, 389 (1999).

[14] F. Graner and Y. Jiang, A physicist's approach to the minimal perimeter problem, in preparation (2000).

[15] F. Elias, C. Flament, J. A. Glazier, F. Graner, and Y. Jiang, Foams out of stable equilibrium: bubble elongation and side swapping, Phil. Mag. B **79** 729–751 (1999).

[16] M. A. Herman and H. Sitter, Molecular Beam Epitaxy, Springer series in material science, 2nd edition, Berlin 1996.

[17] T. Aste, D. Boose, and N. Rivier, From one cell to the whole froth: A dynamical map, Phys. Rev. E **53**, 6181–6191 (1996).

[18] Unless the fluid of edges does not wet the box boundaries, in which case the edges are tangent to the boundaries, see Fig 1b.

[19] H. Foisy et al., Two bubbles with boundaries, preprint, (1999).

[20] M. Asipauskas, Y. Jiang, F. Graner, and J. A. Glazier, in preparation.

[21] G. Schliecker and S. Klapp, Europhys. Lett. **48**, 122–128 (1999).